Scientific Research Publishing

Modern Research in Catalysis, 2020, 9, 1-19
https://www.scirp.org/journal/mrc
ISSN Online: 2168-4499
ISSN Print: 2168-4480

Facile Synthesis of Ag/TiO_2 by Photoreduction Method and Its Degradation Activity of Methylene Blue under UV and Visible Light Irradiation

Hwei-Cheng Tseng, Yu-Wen Chen*

Department of Chemical Engineering, National Central University, Taiwan
Email: *ywchen@cc.ncu.edu.tw

How to cite this paper: Tseng, H.-C. and Chen, Y.-W. (2020) Facile Synthesis of Ag/TiO_2 by Photoreduction Method and Its Degradation Activity of Methylene Blue under UV and Visible Light Irradiation. *Modern Research in Catalysis*, **9**, 1-19.
https://doi.org/10.4236/mrc.2020.91001

Received: November 1, 2019
Accepted: December 14, 2019
Published: December 17, 2019

Abstract

A series of Ag/TiO_2 with various Ag contents were prepared by photoreduction method. Commercial TiO_2 from Evonik-Degussa was used as the catalyst. Ag was used as the cocatalyst. This facial synthesis method is cheap and easy. TiO_2 was suspended in water with various concentrations of silver nitrate. The solution was illuminated by UV light for 36 h. Ag would deposit on the surface of TiO_2. This method can deposit all Ag cation in the starting material on TiO_2 after 36 h irradiation by UV light. X-ray diffraction, high resolution-TEM, and X-ray photoelectron spectroscopy were used to characterize the surface, morphology and chemical composition of the catalysts. Photocatalytic degradation of methylene blue in water on these catalysts was carried out under UV and visible light irradiation, respectively. The methylene blue concentration in water was measured by a UV-vis spectrophotometer. The results showed that the bulk structure of TiO_2 did not change and some of Ag was incorporated into the surface of TiO_2 lattice. The change in the electronic state of Ti on surface is attributed to the replacement of titanium atoms by silver atoms on the TiO_2 surface structure which induced visible light response and enhanced the photocatalytic activity. 1 wt% Ag is the optimum loading to have high activity.

Keywords

Titanium Dioxide, Silver, Photocatalyst, Photoreduction, Photocatalytic Degradation of Methylene Blue

1. Introduction

Titania photocatalyst has been extensively studied in the last two decades [1]-[20]. The TiO_2 from Evonik-Degussa (P25) has been known [1] [2] to have

high photo catalytic activity under UV light irradiation, since it contains both anatase and rutile structure, and the interface between these two phases is the active site. Doping silver on TiO_2 has been known to have plasmon effect and results in high activity under visible light irradiation [3] [4]. It was reported that silver particles can serve as electron traps assisting electron-hole separation. Silver particles also accelerate electron excitation by producing a local electrical field, which can improve the photocatalytic activity of TiO_2 [5]-[12]. Many researchers used sol-gel method and other technique to synthesize $AgTiO_2$. These methods are tedious and costive. In addition, some silver material was lost during preparation. Some researchers used impregnation to prepare $AgTiO_2$, which resulted in big Ag particles.

Generally, surface modification of the semiconductor with noble metal nanoparticles expands the absorption of the semiconductor from UV light to visible light region, due to the surface plasmon resonance absorbance feature, and improves the electron-hole pair separation and consequently the rate of photocatalytic reaction grows [13]-[30]. Noble metal nanoparticles demonstrate strong and wide surface plasmon resonance (SPR) absorption under the visible light owing to the collective oscillations of their conduction band electrons by absorbing visible region. The frequency of the SPR band can be adjusted by modifying the shape and size of the noble metal nanoparticles, which can considerably enlarge the visible-light absorption and can be utilized to exploit efficient plasmonic photocatalysts under visible light. The noble metal nanoparticles are deposited on the surface of semiconductor in the plasmonic photocatalysts, and the metal nanoparticles serve as an element for collecting visible light because of their surface plasmon resonance while the metal-semiconductor interface efficiently departs the photogenerated electrons and holes. As a consequence, several works belonging to the deposition of noble metal nanoparticles such as gold (Au) and silver (Ag) on TiO_2 nanoparticles and their application used as photocatalysts have been fulfilled with great success [27] [28] [29] [30] [31]. The photocatalytic activity of noble metal nanoparticles doped TiO_2 toward the degradation of various environmental pollutants, such as methylene blue, methyl orange, rhodamine blue and 4-cholorophenol, has been well recorded [3] [18]-[33]. However, their photocatalytic efficiency does not arrive the standard demanded for practical applicability. Doping metal on titania can increase active sites and repression of e-/h+ pairs recombination [20]-[45].

The aim of this study was to develop a facile method to prepare Ag/TiO_2, which is simple, low cost and have high activity under UV light and visible light irradiation. The effects of Ag loading on the activity of the catalyst were studied extensively.

2. Experimental

2.1. Materials

Titanium dioxide (P25) was obtained from Evonik Degussa Company. Silver ni-

trate (purity > 99.0%) was from Sigma-Aldrich. Distilled water was used throughout the experiments. Methylene blue (purity > 99.9%) was purchased from Alfa Aesar.

2.2. Catalysts Preparation

Ag/TiO_2 catalysts were prepared by photo-reduction method. TiO_2 was added into a water bath containing various amounts of silver nitrate. It was illuminated under UVC light with stir for 36 h. The catalyst was filter, then dried under vacuum.

2.3. Catalysts Characterization

2.3.1. X-Ray Diffraction (XRD)

XRD patterns of the samples were obtained by a Bruker D2 phaser system, using CuK_α radiation (1.5405 Å) at a voltage and current of 30 kV and 10 mA, respectively. The sample was scanned over the range 2θ = 20˚ - 80˚ at a rate of 0.07˚/min to identify the crystalline structure. The detail has been described in previous literature [5] [6] [7] [8].

2.3.2. High-Resolution Transmission Electron Microscopy (HRTEM)

The observation in morphology and structure of TiO_2 and Ag/TiO_2 particles, including dimension of samples, were investigated by HRTEM on a JEOL JEM-2010 operated at 200 kV. The detail has been described in previous literature [5] [6] [7] [8]. The suspended particles were deposited on the holey carbon-coated copper grid (300#) (Ted Pella). The chemical composition of the samples was determined by Energy-dispersive X-ray spectroscopy (EDS) attached on the HRTEM with accelerating voltage of 200 kV, and using silicon detector.

2.3.3. X-Ray Photoelectron Spectroscopy (XPS)

The XPS spectra of the samples were recorded with a Thermo VG Scientific Sigma Prob spectrometer. The detail has been described in previous literature [5] [6] [7] [8]. The XPS spectra were collected using Al Kα radiation at a voltage and current of 20 kV and 30 mA, respectively. The base pressure in the analyzing chamber was maintained in the order of 10^{-7} Pa. The pass energy was 23.5 eV and the binding energy was calibrated by contaminant carbon (C_{1S} = 284.5 eV). The peaks of each spectrum were organized using XPSPEAK software; Shirley type background and 30:70 Lorentzian/Gaussian peak shape were used for deconvolution of the spectra.

2.4. Photocatalytic Degradation of Methylene Blue

In this study, the decomposition of methylene blue in aqueous solution under both UV light and visible light irradiation was used as the standard testing reaction. The detail has been described in previous literature [5] [6] [7] [8]. For the photocatalytic activity reaction, the catalyst was activated for 12 h by four pieces of 9 W UV lamps (wavelength = 254 nm (UVC), TUV PL-L 18W/4P 1CT/25, Philips). This procedure can photoreduce AgO to Ag metal completely. 40 mL of

methylene blue aqueous solution with the concentration of 10 mg/L was held in quartz cell. The catalyst was added into the solution. Before the photocatalytic reaction was conducted, the reactor was held in the dark place for 1 h for the saturation adsorption of MB. The catalyst was then illuminated by four 9 W UV lamps (254 nm wavelength, TUV PL-L 18W/4P 1CT/25, Philips) or four 9 W visible light lamps (Master PL-L 18W/840/4P, Philips). The distance from the lamps to the surface of the solution was 10 cm, and the concentration of MB in aqueous solution was determined every 15 min for UV light reaction or every 1 h for visible light reaction by using UV-vis spectroscopy (Jasco V-670). The concentration of MB was determined by the intensity of 663 nm adsorption peak, which is the characteristic UV-vis peak of MB.

3. Results and Discussion

3.1. XRD

The crystalline structures of TiO_2 and Ag/TiO_2 were characterized by XRD. All of the diffraction peaks of the samples, as shown in **Figure 1**, are located at the same positions [5] [6] [7] [8] [35]-[45]. The diffraction peaks located at 2θ = 25.31˚, 37.80˚, 48.05˚, 53.89˚, 55.06˚, 62.69˚, 68.76˚, 75.03˚ corresponding to the anatase form of (101), (004), (200), (105), (211), (204), (116) and (215) (JCPDS 21-1272). The diffraction peaks located at 2θ = 27.44˚, 36.09˚, 54.32˚, 56.63˚, 64.06˚, 69.01˚, 69.80˚ corresponding to the rutile form of (110), (101), (211), (220), (310), (301) and (112) (JCPDS 34-0180). P25 TiO_2 from Evonik Degussa contains both anatase and rutile crystalline phases, addition of Ag did not change bulk crystalline structure, as expected. The peak of silver was not observed, implying that the particle size of silver was very small. The crystallite size

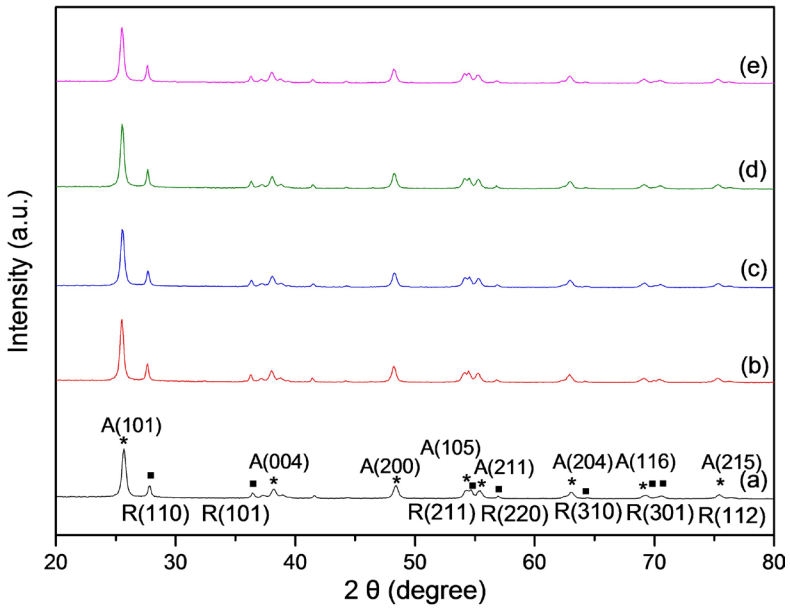

Figure 1. The XRD patterns of (a) TiO_2, (b) $0.5Ag/TiO_2$, (c) $1Ag/TiO_2$, (d) $1.5Ag/TiO_2$, (e) $2Ag/TiO_2$. (*represent the anatase form; ▪represent the rutile form).

and d-spacing of TiO_2 were calculated by using the Debye-Scherrer equation and the Bragg's law, respectively. The results are listed in Table 1. It should be noted that silver addition did not change the crystallite size of TiO_2, indicating the distortion of the crystal lattice by incorporation of Ag ions was only into surface of TiO_2. It did not change the bulk structure of TiO_2.

3.2. HR-TEM

The morphology of the as-prepared catalyst was investigated by HR-TEM. Figure 2 shows that AgO particles were spherical shape, and the lattice spacing was 0.241 nm, in consistent with (111) plane of silver oxide.

Figure 3 shows the HRTEM of all the Ag/TiO_2 samples. It clearly shows that AgO was deposited on the surface of TiO_2. The particle of TiO_2 from Evonik Degussa is cubic and the size is about 5 nm. The size of AgO should be less than 5 nm. Some of AgO agglomerated on the surface of TiO_2. When Ag^+ was deposited on TiO_2 after photoreduction preparation process, Ag^+ was photoreduced to Ag^0. The sample was exposed to air after preparation. Ag^0 would be oxidized to AgO. When the sample was in HRTEM chamber, even under high vacuum, it was still in AgO state. The HRTEM shows the AgO spacing in all the samples.

3.3. XPS

The XPS spectra in the Ti 2p region of the samples are shown in Figure 4. The

Table 1. The crystallite size and d-spacing of TiO_2 in Ag/TiO_2 catalysts.

As-prepared powder	Crystallite size (nm)	d-spacing (nm)
TiO_2	21.86	0.352
$0.5Ag/TiO_2$	21.86	0.352
$1Ag/TiO_2$	21.86	0.352
$1.5Ag/TiO_2$	21.86	0.352
$2Ag/TiO_2$	21.86	0.352

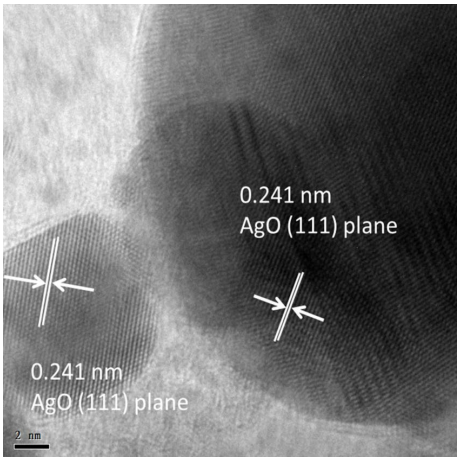

Figure 2. The HRTEM image of the P-Ag/TiO_2 particles showing the lattice spacing of silver oxide.

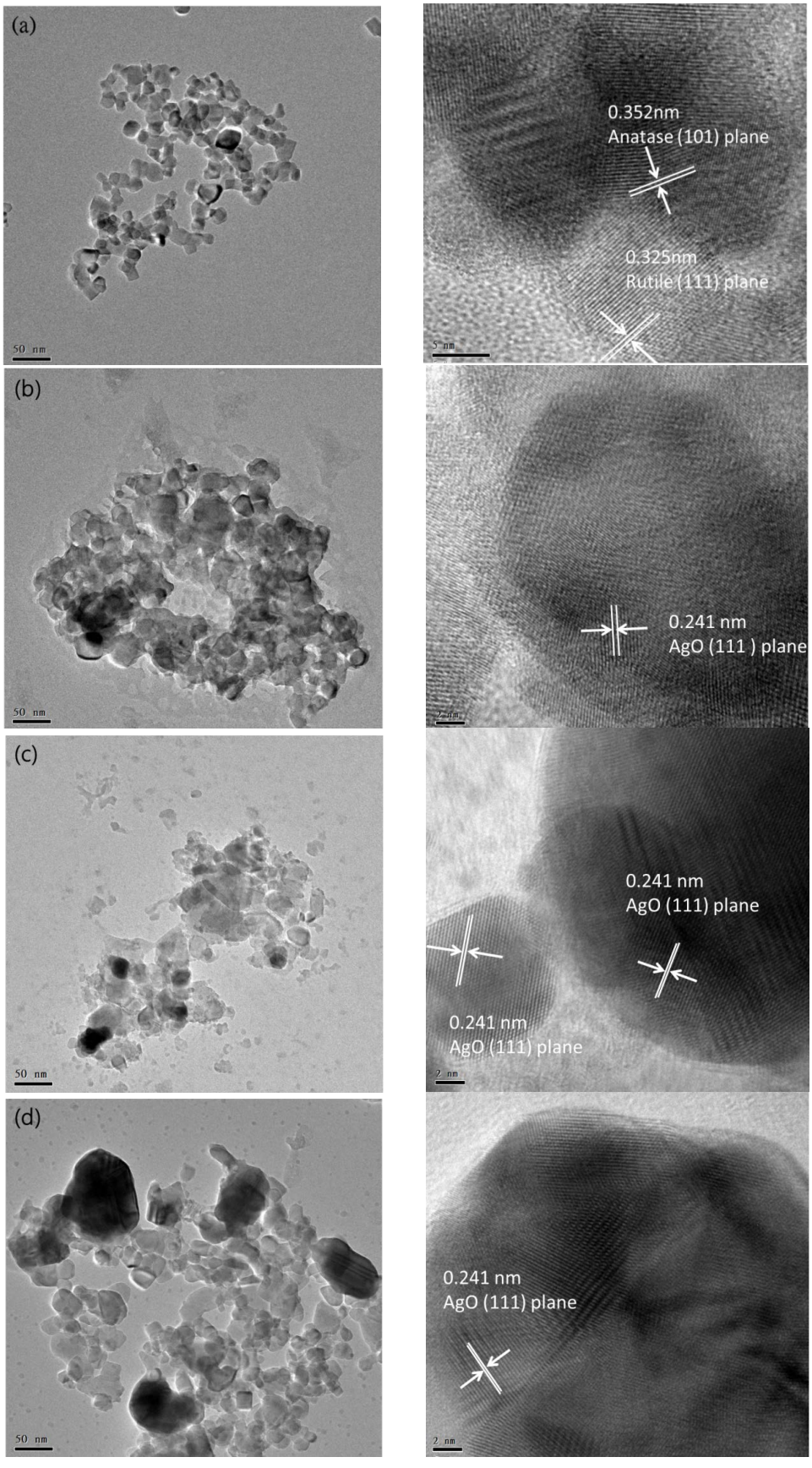
(a)
50 nm
0.352nm
Anatase (101) plane
0.325nm
Rutile (111) plane
5 nm
(b)
50 nm
0.241 nm
AgO (111) plane
2 nm
(c)
50 nm
0.241 nm
AgO (111) plane
0.241 nm
AgO (111) plane
2 nm
(d)
50 nm
0.241 nm
AgO (111) plane
2 nm

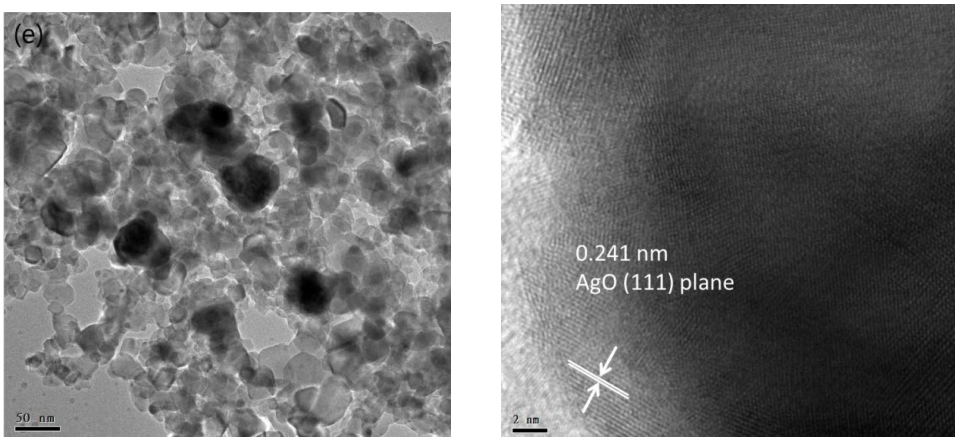

Figure 3. The HRTEM images of (a) TiO_2, (b) 0.5Ag/TiO_2, (c) 1Ag/TiO_2, (d) 1.5Ag/TiO_2, and (e) 2Ag/TiO_2.

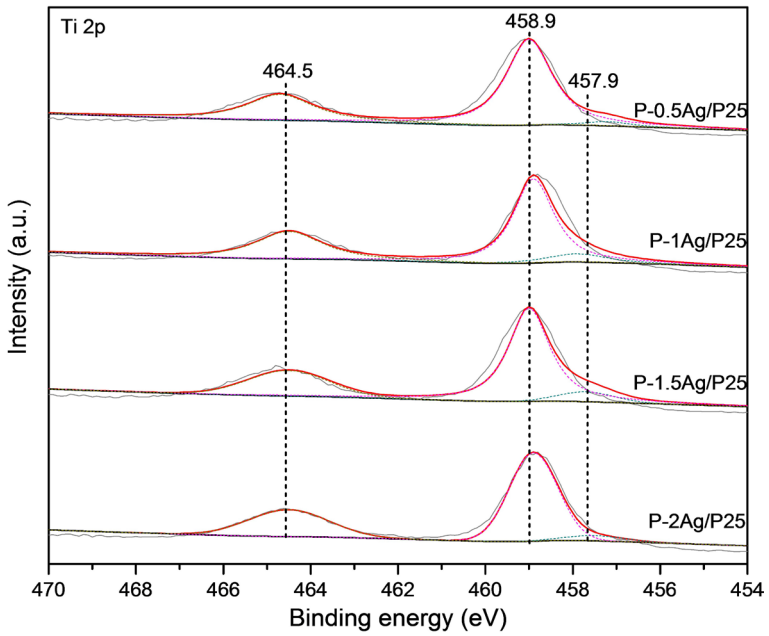

Figure 4. XPS spectra of Ti 2p region of Ag/TiO_2 powders.

peaks located at binding energy of 458.9 - 459.0 eV corresponds to Ti $2p_{3/2}$ state and at 464.5 - 464.7 eV corresponds to Ti $2p_{1/2}$ state [5]-[10]. It is attributed to the Ti^{4+} in TiO_2 lattice. It shows that the Ti $2p_{3/2}$ peaks were broadened with increasing silver content of the sample. The results indicate that the valence state of Ti cation was reduced from Ti^{4+} to Ti^{3+} by charge compensation and the silver could trap the electrons, which decreased the recombination rate of electrons and holes and convert more Ti^{4+} ions to Ti^{3+} ions [33] [34] [35] [36]. The generation of Ti^{3+} ions could induce visible light response by the creation of oxygen vacancies [38]-[45].

Table 2 shows the fractions of Ti^{3+} and Ti^{4+}, respectively, in each sample. Pure TiO_2 is fully crystallized, and the fraction of Ti^{3+} is zero. After loading Ag, the fraction of Ti^{3+} was not zero. Since the Ag content was very low, and only part of

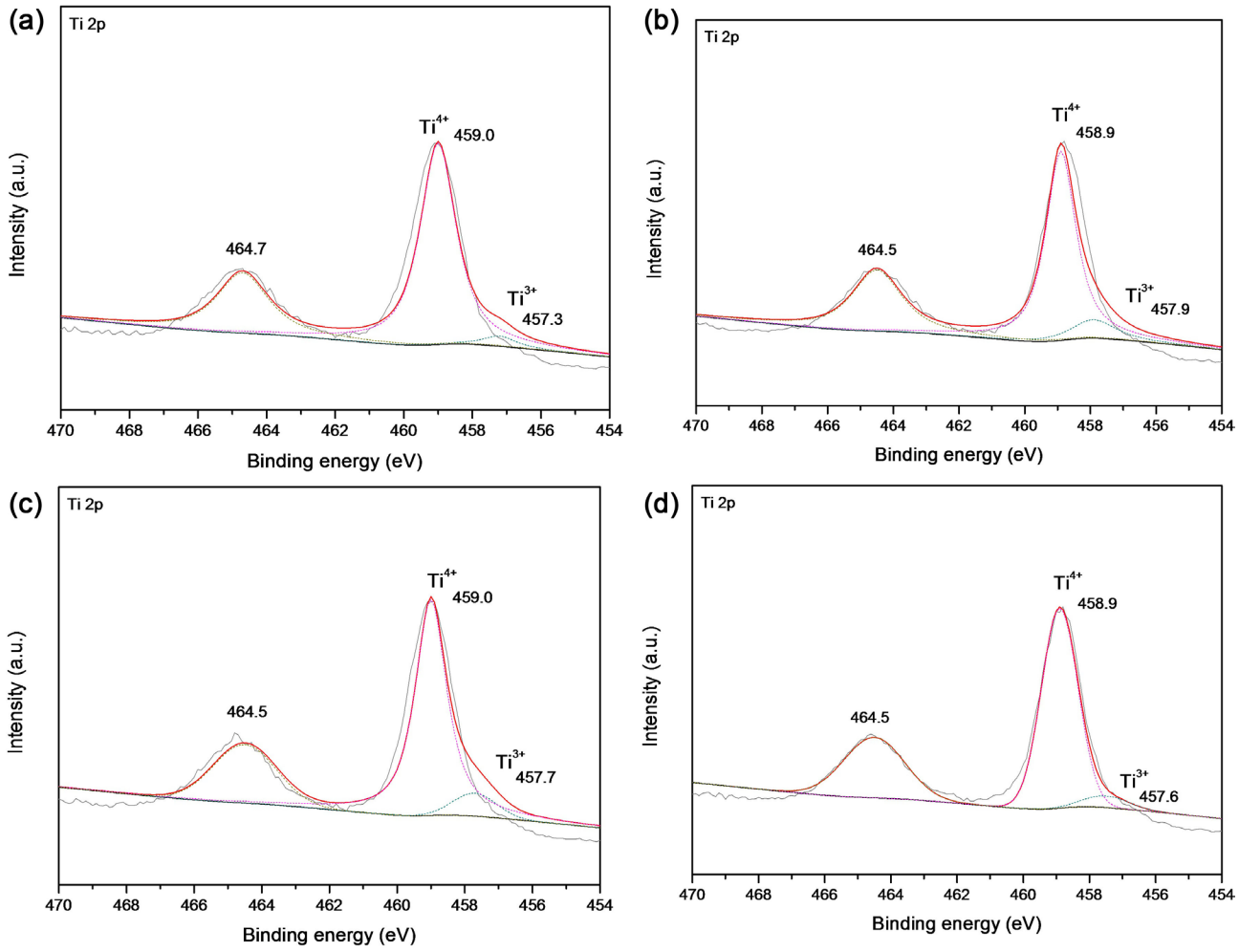

Figure 5. XPS spectra of Ti $2p_{3/2}$ region of (a) 0.5Ag/TiO_2, (b) 1Ag/TiO_2, (c) 1.5Ag/TiO_2, (d) 2Ag/TiO_2.

Table 2. Ti $2p_{3/2}$ XPS data and the fraction of total area of Ag/TiO_2.

catalyst	Ti^{3+}		Ti^{4+}	
	B.E. (eV)	Fraction (%)	B.E. (eV)	Fraction (%)
0.5Ag/TiO_2	457.3	3.84	459.0	97.16
1Ag/TiO_2	457.9	8.41	458.9	91.59
1.5Ag/TiO_2	457.7	7.08	459.0	92.92
2Ag/TiO_2	457.6	4.57	458.9	95.43

Ag was incorporated into surface structure of TiO_2. The fraction of Ti^{3+} was low. Nevertheless, it clears shows that the fraction of Ti^{3+} increased after loading with Ag. The 2Ag/TiO_2 sample had lower fraction of Ti^{3+} compared with 1Ag/TiO_2, possibly because Ag was agglomerated to form big particles, resulting in small amount of Ag was incorporated into surface structure of TiO_2. Further studies are needed to investigate this phenomenon.

Figure 6 and Figure 7 display the XPS spectra of the O 1s region of Ag/TiO_2 catalysts. Two O 1s peaks appeared in both samples, which is ascribed to lattice

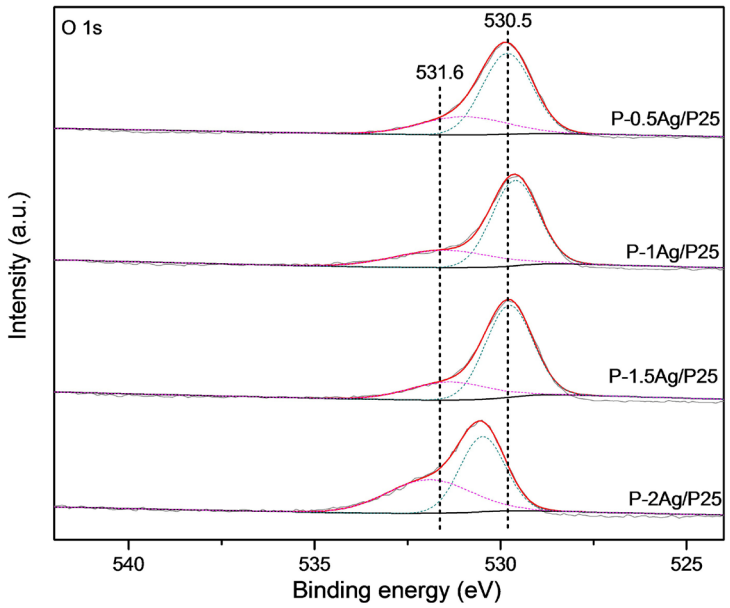

Figure 6. XPS spectra of O 1s region of Ag/TiO_2.

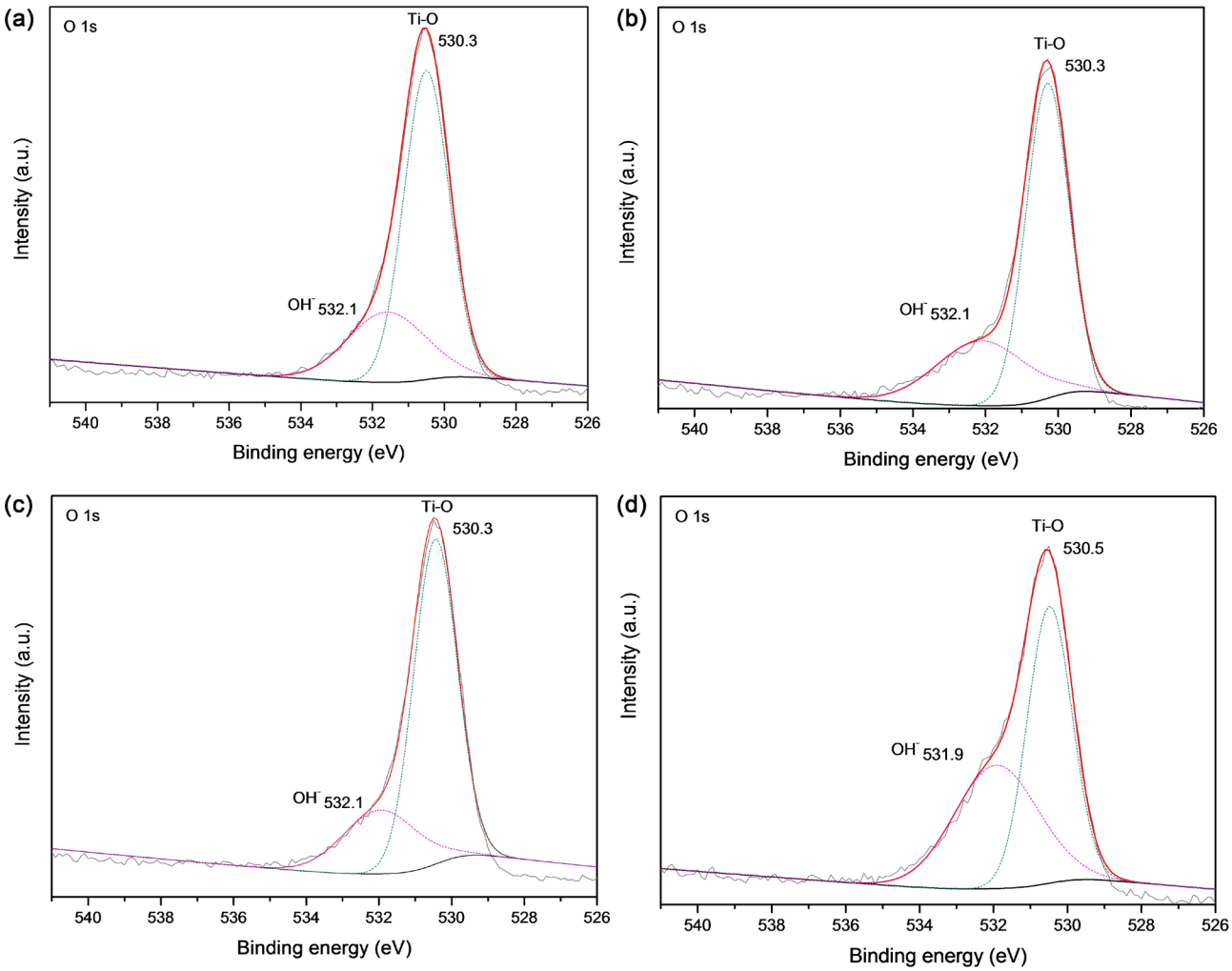

Figure 7. XPS spectra of O 1s region of (a) $0.5Ag/TiO_2$, (b) $1Ag/TiO_2$, (c) $1.5Ag/TiO_2$, (d) $2Ag/TiO_2$.

oxygen for Ti-O bond and hydroxyl groups on the surface [7]-[13] [38]-[45], respectively. The Ag/TiO_2 could generate more active hydroxyl radicals (HO·), which is the major species for degradation of methylene blue [38]-[45].

Figure 8 and Figure 9 show the XPS spectra of Ag 3d. The XPS curve can be well fitted by two peaks centered at 367.8 eV and 373.8 eV corresponding to silver oxide, respectively [41] [42] [43] [44] [45]. Before reaction, the catalyst was irradiated by UV light overnight. Under such condition, AgO was photoreduced to Ag metal. It is known that Ag nanoparticles could improve the photocatalytic efficiency via the following ways:

$$Ag^0 + e^- \rightarrow Ag^- \quad (1)$$

$$Ag^- + O_2 \rightarrow O_2^{\cdot -} + Ag^0 \quad (2)$$

The Ag nanoparticles were used as surface traps which can capture the electrons from the conduction of TiO_2 and inhibit the electron/hole pair recombination [38]-[44]. These electrons further move from conduction of TiO_2 to the Ag nanoparticles and react with the dissolve oxygen to generate the superoxide

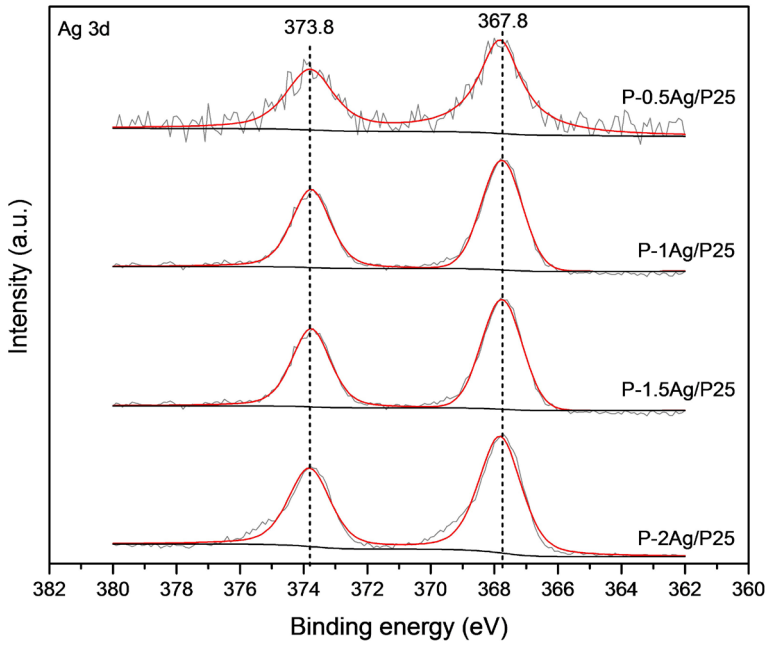

Figure 8. XPS spectra of O 1s region of (a) $0.5Ag/TiO_2$, (b) $1Ag/TiO_2$, (c) $1.5Ag/TiO_2$, (d) $2Ag/TiO_2$.

Table 3. O 1s XPS data and the fraction of total area of Ag/TiO_2.

As-prepared powder	lattice O^{2-}		Hydroxyl group on surface	
	B.E. (eV)	Fraction (%)	B.E. (eV)	Fraction (%)
$0.5Ag/TiO_2$	530.3	71.72	532.1	28.28
$1Ag/TiO_2$	530.3	69.87	532.1	30.13
$1.5Ag/TiO_2$	530.3	74.97	532.1	25.03
$2Ag/TiO_2$	530.5	54.45	531.9	45.55

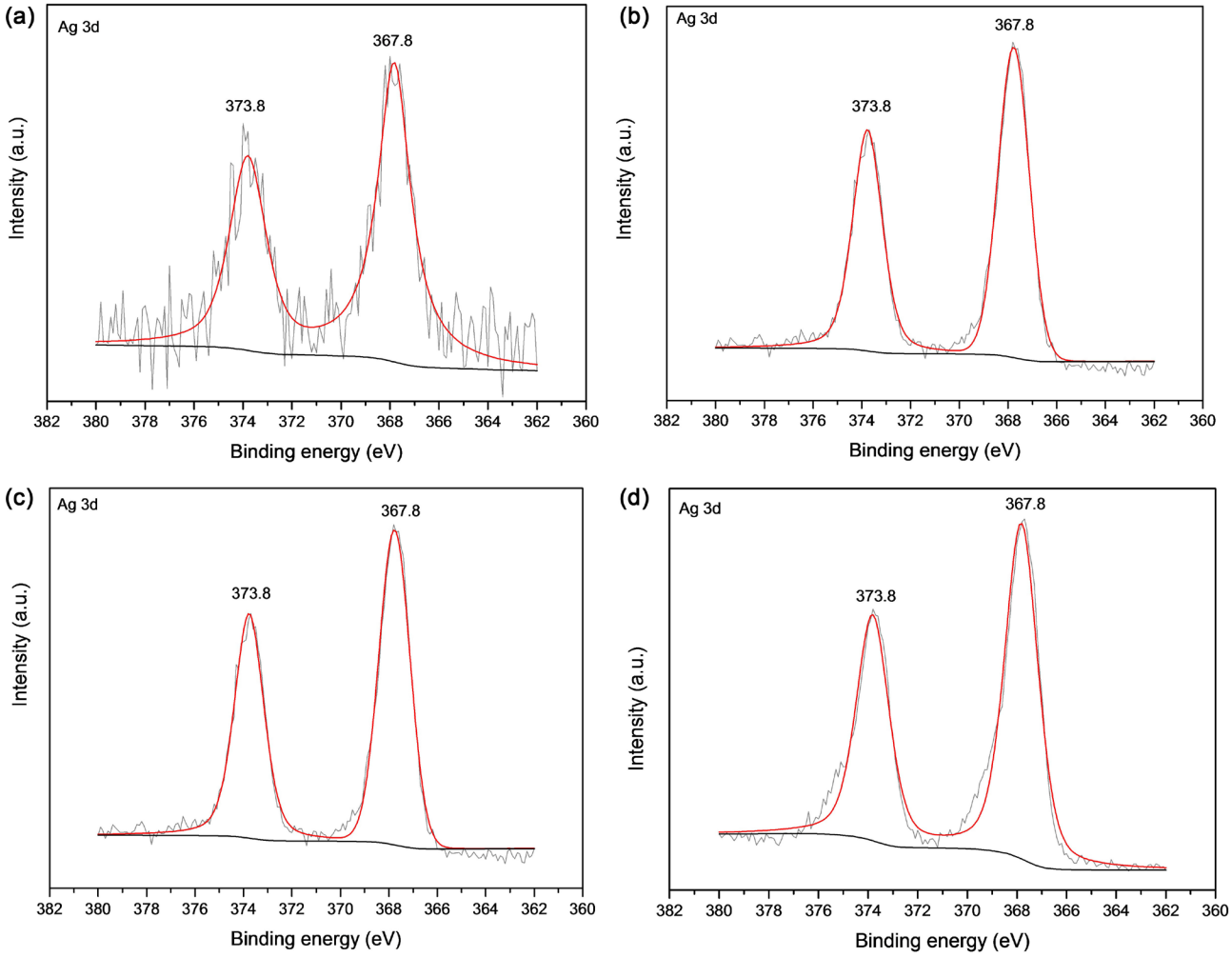

Figure 9. XPS spectra of Ag 3d region of (a) 0.5Ag/TiO_2, (b) 1Ag/TiO_2, (c) 1.5Ag/TiO_2, (d) 2Ag/TiO_2.

radical anions ($O_2^{\bullet -}$).

3.4. Photocatalytic Degradation of Methylene Blue Aqueous Solution

Figure 10 shows the adsorption amount of methylene blue on the catalyst. The amount of methylene blue adsorption increased after loading silver concentration. Multilayer methylene blue was adsorbed on the surface of catalyst, indication that adsorption of methylene blue is not the rate-determining step.

The results of photocatalytic activity under UV light irradiation are shown in Figure 11. It can be seen that the 1Ag/TiO_2 had the highest activity among all of the samples under UV light illumination. The photocatalytic activity of Ag/TiO_2 decreased when the silver content was more than 1 wt%. As silver concentration is more than the optimum amount, Ag becomes the recombination center of the photo-induced electrons and holes, which is harmful for photocatalytic reactions.

The photodegradation of organic dyes is suited to the Langmuir–Hinshelwood model. The slope of $\ln(C_0/C)$ plotted versus irradiation time (min or h) demonstrates the rate constant of the reaction of the sample, as shown in Figure 12.

The rate constants of catalysts for destructure of methylene blue are calculated and listed in Table 4. The reaction rate constant of 1Ag/TiO_2 was 0.64964 h^{-1} which was about four times of that of pure TiO_2.

Figure 13 shows the results of photocatalytic activity under visible light illumination. The photocatalytic activities of all of the Ag/TiO_2 had improvements compared to the pure P25 powder since adding Ag could have plasmon effect.

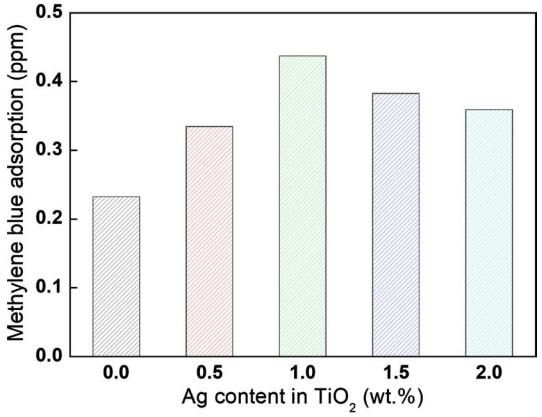

Figure 10. The methylene blue adsorption of Ag/TiO_2 powders under UV light irradiation.

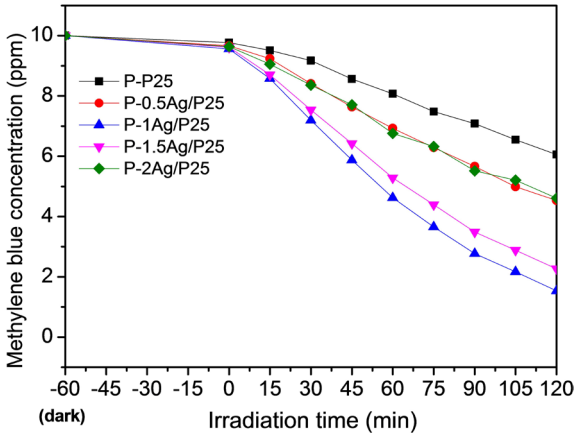

Figure 11. Photocatalytic degradation of methylene blue of Ag/TiO_2 under UV light irradiation.

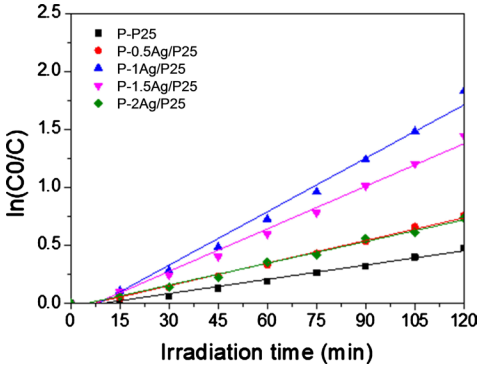

Figure 12. Photocatalytic activities of Ag/TiO_2 under UV light irradiation by plotting $\ln(C_0/C)$ versus irradiation time (min).

Table 4. Rate constant (h^{-1}) of reactions of Ag/TiO_2 under UV light irradiation.

As-prepared powder	Rate constant (k, h^{-1})
TiO_2	0.17540
$0.5Ag/TiO_2$	0.39409
$1Ag/TiO_2$	0.64964
$1.5Ag/TiO_2$	0.53829
$2Ag/TiO_2$	0.29812

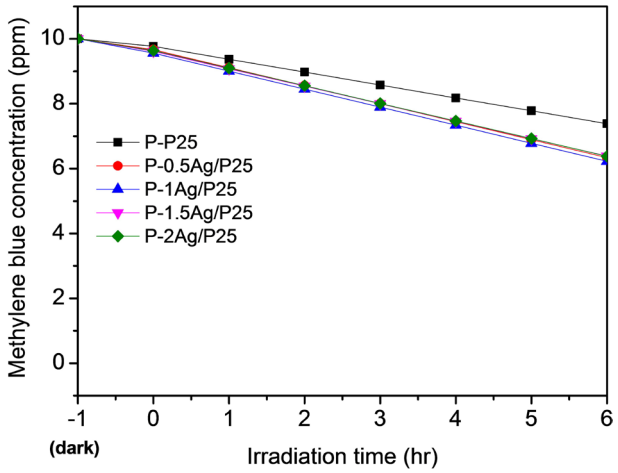

Figure 13. Photocatalytic degradation of methylene blue of P-Ag/TiO_2 P25 powders under visible light irradiation.

Consequently, the synthesized powders can have higher photocatalytic activity under visible light illumination [38] [39] [40]. In addition, the samples would decrease Ti^{4+} ions to Ti^{3+} ions by charge compensation and the generation of Ti^{3+} ions could induce visible light response by the creation of oxygen vacancies which were consistent with the XPS spectra analysis for Ti 2p region [29] [30] [38] [39] [40]. As shown in **Figure 14** and **Table 5**, the photocatalytic activity of Ag/TiO_2 was the highest among all catalysts under visible light irradiation. The rate constant of the reaction was calculated to be 0.059911 h^{-1} which had the most hydroxyl groups in all samples.

$1Ag/TiO_2$ showed the highest photocatalytic activity among all catalysts under UV light and visible light illumination since degradation by TiO_2 was conducted prominent via ·OH radicals generated in the positive holes, while Ag/TiO_2 catalysts generated ·OH radicals through the transformation of $O_2^{\bullet-}$ radicals [29] [30].

It has been reported [13] [14] [15] that the Fermi level of TiO_2 is higher than that of doped silver. Consequently, silver deposits behave like accumulation sites for photogenerated electrons moved from TiO_2. As the number of silver cluster is small and the electrons efficiently move to silver cluster, better separation of electrons and holes would be complied with increment of silver doping to the optimum content. The electrons could react with surface Ti^{4+} or adsorbed oxygen molecular to produce reactive center surface Ti^{3+} and reactive species

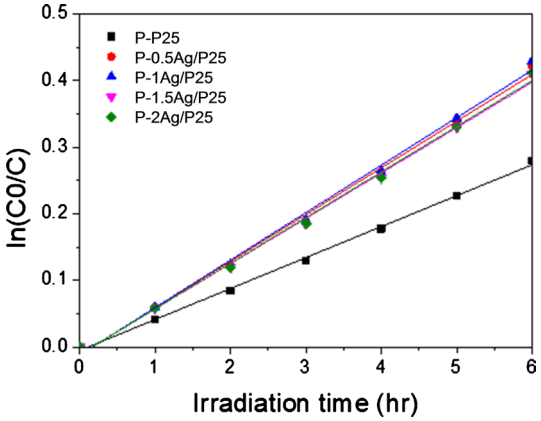

Figure 14. Photocatalytic activities of P-Ag/TiO_2 powders under visible light irradiation by plotting $\ln(C_0/C)$ versus irradiation time (h).

Table 5. Rate constant (h^{-1}) of reactions of Ag/TiO_2 under visible light irradiation.

Catalyst	Rate constant (k, h^{-1})
TiO_2	0.0415
0.5Ag/TiO_2	0.0591
1Ag/TiO_2	0.0599
1.5Ag/TiO_2	0.0577
2Ag/TiO_2	0.0580

$O_2^{\bullet-}$, respectively, the deal of recombination center of inner Ti^{3+} reduced at the same time. Furthermore, the doped silver particle can move an electron to adsorbed oxygen molecular to produce $O_2^{\bullet-}$ or to the TiO_2 surface Ti^{4+} to produce surface Ti^{3+}. This indicated that the recombination was slowed and the production of $O_2^{\bullet-}$ and surface Ti^{3+} was speeded up. The productivity of h^+ would also be raised. The reactions are shown as follows:

$$e^- + Ag_n \rightarrow Ag_n^- \quad (3)$$

$$Ag_n^- + O_2 \rightarrow Ag_n + O_2^{\bullet-} \quad (4)$$

$$Ag_n^- + Ti^{4+} \rightarrow Ag_n + Ti^{3+}_{surface} \quad (5)$$

With increment of silver doping, the quantity and size of silver cluster became bigger progressively and the energetic properties of the doped silver may be closed to that of bulk silver making the silver sites turn into recombination center of electrons and holes.

$$Ag_n^- + h^+ \rightarrow Ag_n \quad (6)$$

Moreover, higher amount of silver would enshroud more TiO_2 surface and prevent the contact between organics and TiO_2, which would decrease lots of received photons and increase diffuse distance.

4. Conclusions

A series of Ag/TiO_2 were prepared by photoreduction method. The samples were

characterized by XRD, HR-TEM, and XPS. The photocatalytic activity of the samples was examined by the methylene blue degradation under UV light and visible light illumination, respectively.

XRD patterns show that anatase and rutile forms were present among all of the samples. The XRD peak of silver oxide was not observed, implying that the particle size of AgO was very small. Doping silver would generate more Ti^{3+} ions on the surface that could induce UV and visible light response by the creation of oxygen vacancies and generate more active hydroxyl radicals which are the major species for degradation of organic dye.

1 wt% Ag/TiO_2 demonstrated the highest photocatalytic activity among all catalysts under both UV light and visible light illumination for the degradation of methylene blue dye.

The advantages of using photoreduction to prepare Ag/TiO_2 are as following. 1) All of Ag cations in starting material could be deposited and reduced on TiO_2 surface; 2) TiO_2 is commercially available and is cheap; 3) the bulk structure of TiO_2 is fully crystallized, and only surface structure is changed, resulting in high photocatalytic activities; 4) the preparation method is simple.

Acknowledgements

This research was financially supported by the Ministry of Science and Technology, Taiwan.

Conflicts of Interest

The authors declare no conflicts of interest regarding the publication of this paper.

References

[1] Sanzone, G., Zimbone, M., Cacciato, G., Ruffino, F., Carles, R., Privitera, V. and Grimaldi, M.G. (2018) Ag/TiO_2 Nanocomposite for Visible Light-Driven Photocatalysis. *Superlattices and Microstructures*, **123**, 394-402. https://doi.org/10.1016/j.spmi.2018.09.028

[2] Noreen, Z., Khalid, N.R., Abbasi, R., Jayed, S., Ahmad, I. and Bokhari, H. (2019) Visible Light Sensitive Ag/TiO_2/Graphene Composite as a Potential Coating Material for Control of *Campylobacter jejuni*. *Materials Science and Engineering*: *C*, **98**, 125-133. https://doi.org/10.1016/j.msec.2018.12.087

[3] Zhang, Y., Fu, F., Li, Y., Zhang, D. and Chen, Y. (2018) One-Step Synthesis of Ag@TiO_2 Nanoparticles for Enhanced Photocatalytic Performance. *Nanomaterials*, **8**, 1032-1042. https://doi.org/10.3390/nano8121032

[4] Chan, S.C. and Barteau, M.A. (2005) Preparation of Highly Uniform Ag/TiO_2 and Au/TiO_2 Supported Nanoparticle Catalysts by Photodeposition. *Langmuir*, **21**, 5588-5595. https://doi.org/10.1021/la046887k

[5] Moongraksathum, B. and Chen, Y.W. (2017) CeO_2-TiO_2 Mixed Oxide Thin Films with Enhanced Photocatalytic Degradation of Organic Pollutants. *Journal of Sol-Gel Science and Technology*, **82**, 772-782. https://doi.org/10.1021/la046887k

[6] Moongraksathum, B. and Chen, Y.W. (2018) Anatase TiO_2 Co-Doped with Silver

and Ceria for Antibacterial Application. *Catalysis Today*, **310**, 69-74. https://doi.org/10.1016/j.cattod.2017.05.087

[7] Moongraksathum, B., Shang, J.Y. and Chen, Y.W. (2018) Photocatalytic Antibacterial Effectiveness of Cu-Doped TiO_2 Thin Film Prepared via Peroxo Sol-Gel Method. *Catalysts*, **8**, 352-361. https://doi.org/10.3390/catal8090352

[8] Moongraksathum, B., Chien, M.Y. and Chen, Y.W. (2019) Antiviral and Antibacterial Effects of Silver-Doped TiO_2 Prepared by the Peroxo Sol-Gel Method. *Journal of Nanoscience and Nanotechnology*, **19**, 1-7. https://doi.org/10.1166/jnn.2019.16615

[9] Rather, R.A., Singh, R. and Pal, B. (2017) Visible and Direct Sunlight Induced H2 Production from Water by Plasmonic Ag-TiO_2 Nanorods Hybrid Interface. *Solar Energy Materials and Solar Cells*, **160**, 463-469. https://doi.org/10.1016/j.solmat.2016.11.017

[10] Liu, X., Iocozzia, J., Wang, Y., Cui, X., Chen, Y., Zhao, L., Li, Z. and Lin, Z. (2017) Noble Metal-Metal Oxide Nanohybrids with Tailored Nanostructures for Efficient Solar Energy Conversion, Photocatalysis and Environmental Remediation. *Energy & Environmental Science*, **10**, 402-434. https://doi.org/10.1039/C6EE02265K

[11] Cao, C., Huang, J., Li, L., Zhao, C. and Yao, J. (2017) Highly Dispersed Ag/TiO_2 via Adsorptive Self-Assembly for Bactericidal Application. *RSC Advances*, **7**, 13347-13352. https://doi.org/10.1039/C7RA00758B

[12] Xie, Y., Huang, Z., Zhang, Z., Zhang, X., Wen, R., Liu, Y., Fang, M. and Wu, X. (2016) Controlled Synthesis and Photocatalytic Properties of Rhombic Dodecahedral Ag_3PO_4 with High Surface Energy. *Applied Surface Science*, **389**, 56-66. https://doi.org/10.1016/j.apsusc.2016.07.088

[13] Jia, C., Yang, P., Li, J., Huang, B. and Matras-Postolek, K. (2016) Photocatalytic Activity Evolution of Different Morphological TiO_2 Shells on Ag Nanowires. *ChemCatChem*, **8**, 839-847. https://doi.org/10.1002/cctc.201501045

[14] Kenens, B., Chamtouri, M., Aubert, R., Miyakawa, K., Hayasaka, Y., Naiki, H., Watanabe, H., Inose, T., Fujita, Y., Lu, G., Masuhara, A. and Uji-I, H. (2016) Solvent-Induced Improvement of Au Photo-Deposition and Resulting Photo-Catalytic Efficiency of Au/TiO_2. *RSC Advances*, **6**, 97464-97468. https://doi.org/10.1039/C6RA19372B

[15] Rao, Y.N., Banerjee, D., Datta, A., Das, S.K. and Saha, A. (2016) Low Temperature Synthesis of Ag@anatase TiO_2 Nanocomposites through Controlled Hydrolysis and Improved Degradation of Toxic Malachite Green under Both Ultra-Violet and Visible Light. *RSC Advances*, **6**, 49083-49090. https://doi.org/10.1039/C6RA05579F

[16] Zhang, H., Tao, Z., Tang, Y., Yang, M. and Wang, G. (2016) One-Step Modified Method for a Highly Efficient Au-PANI@TiO_2 Visible-Light Photocatalyst. *New Journal of Chemistry*, **40**, 8587-8592. https://doi.org/10.1039/C6NJ02408D

[17] Devi, L.G. and Kavitha, R. (2016) A Review on Plasmonic Metal/TiO_2 Composite for Generation, Trapping, Storing and Dynamic Vectorial Transfer of Photogenerated Electrons across the Schottky Junction in a Photocatalytic System. *Applied Surface Science*, **360**, 601-622. https://doi.org/10.1016/j.apsusc.2015.11.016

[18] Wang, X., Wang, Z., Jiang, X., Tao, J., Gong, Z., Cheng, Y., Zhang, M., Yang, L., Lv, J., He, G. and Sun, Z. (2016) Silver-Decorated TiO_2 Nanorod Array Films with Enhanced Photoelectrochemical and Photocatalytic Properties. *Journal of the Electrochemical Society*, **163**, H943-H950. https://doi.org/10.1149/2.0551610jes

[19] Maparu, A.K., Ganvir, V. and Rai, B. (2015) Titania Nanofluids with Improved Photocatalytic Activity under Visible Light. *Colloids and Surfaces A*: *Physicochem-*

ical and Engineering Aspects, **482**, 345-352.
https://doi.org/10.1016/j.colsurfa.2015.06.026

[20] Zhu, Y., Yang, S., Cai, J., Meng, M. and Li, X. (2015) A Facile Synthesis of Ag-$_x$Au$_{1-x}$/TiO$_2$ Photocatalysts with Tunable Surface Plasmon Resonance (SPR) Frequency Used for RhB Photodegradation. *Materials Letters*, **154**, 163-166.
https://doi.org/10.1016/j.matlet.2015.04.091

[21] Ma, J., Guo, S., Guo, X. and Ge, H. (2015) Modified Photodeposition of Uniform Ag Nanoparticles on TiO$_2$ with Superior Catalytic and Antibacterial Activities. *Journal of Sol-Gel Science and Technology*, **75**, 366-373.
https://doi.org/10.1007/s10971-015-3709-1

[22] Wang, A., Yu, W., Fang, Y., Song, Y., Jia, D., Long, L., Cifuentes, M.P., Humphrey, M.P. and Zhang, C. (2015) Facile Hydrothermal Synthesis and Optical Limiting Properties of TiO$_2$-Reduced Graphene Oxide Nanocomposites. *Carbon*, **89**, 130-141. https://doi.org/10.1016/j.carbon.2015.03.037

[23] Wang, Z. and Zhu, Y. (2015) A Simple Plasma Reduction for Synthesis of Au and Pd Nanoparticles at Room Temperature. *Chinese Journal of Chemical Engineering*, **23**, 1060-1063. https://doi.org/10.1016/j.cjche.2014.09.055

[24] Lu, Y., Zhang, Y., Zhi, Q., Wang, Q., Gittleson, F.S., Li, J. and Taylor, A.D. (2015) Enhanced Photoelectrochemical and Sensing Performance of Novel TiO$_2$ Arrays to H$_2$O$_2$ Detection. *Sensors and Actuators B*: *Chemical*, **211**, 111-115.
https://doi.org/10.1016/j.snb.2015.01.060

[25] Ma, X., Guo, X., Zhang, Y. and Ge, H. (2014) Catalytic Performance of TiO$_2$@Ag Composites Prepared by Modified Photodeposition Method. *Chemical Engineering Journal*, **258**, 247-253. https://doi.org/10.1016/j.cej.2014.06.120

[26] Rodríguez, J.L., Valenzuela, M.A., Tiznado, H., Poznyak, T. and Flores, E. (2014) Synthesis of Nickel Oxide Nanoparticles Supported on SiO$_2$ by Sensitized Liquid Phase Photodeposition for Applications in Catalytic Ozonation. *Journal of Molecular Catalysis A*: *Chemical*, **392**, 39-49. https://doi.org/10.1016/j.molcata.2014.04.028

[27] Jiang, B., Peng, X., Qu, Y., Wang, H., Tian, C., Pan, Q., Li, M., Zhou, W. and Fu, H. (2014) A New Combustion Route to Synthesize Mixed Valence Vanadium Oxide Heterojunction Composites as Visible-Light-Driven Photocatalysts. *ChemCatChem*, **6**, 2553-2559. https://doi.org/10.1002/cctc.201402336

[28] DuChene, J.S., Sweeny, B.C., Johnston-Peck, A.C., Su, D., Stach, E.A. and Wei, W.D. (2014) Prolonged Hot Electron Dynamics in Plasmonic-Metal/Semiconductor Heterostructures with Implications for Solar Photocatalysis. *Angewandte Chemie*, **126**, 8021-8025. https://doi.org/10.1002/ange.201404259

[29] DuChene, J.S., Sweeny, B.C., Johnston-Peck, A.C., Su, D., Stach, E.A. and Wei, W.D. (2014) Prolonged Hot Electron Dynamics in Plasmonic-Metal/Semiconductor Heterostructures with Implications for Solar Photocatalysis. *Angewandte Chemie International Edition*, **53**, 7887-7891. https://doi.org/10.1002/anie.201404259

[30] An, Y., Yang, L., Hou, J., Liu, Z. and Peng, B. (2014) Synthesis and Characterization of Carbon Nanotubes-Treated Ag@TiO$_2$ Core-Shell Nanocomposites with Highly Enhanced Photocatalytic Performance. *Optical Materials*, **36**, 1390-1395.
https://doi.org/10.1016/j.optmat.2014.03.038

[31] Wang, H., Yang, K.F., Li, L., Bai, Y., Zheng, Z.J., Zhang, W.Q., Gao, Z.W. and Xu, L.W. (2014) Modulation of Silver-Titania Nanoparticles on Polymethylhydrosiloxane-Based Semi-Interpenetrating Networks for Catalytic Alkynylation of Trifluoromethyl Ketones and Aromatic Aldehydes in Water. *ChemCatChem*, **6**, 580-591.
https://doi.org/10.1002/cctc.201300870

[32] Lee, W.S., Park, Y.S. and Cho, Y.K. (2014) Significantly Enhanced Antibacterial Activity of TiO_2 Nanofibers with Hierarchical Nanostructures and Controlled Crystallinity. *The Analyst*, **140**, 616-622. https://doi.org/10.1039/C4AN01682C

[33] Khanna, A. and Shetty, V.K. (2014) Solar Light Induced Photocatalytic Degradation of Reactive Blue 220 (RB-220) Dye with Highly Efficient Ag@TiO_2 Core-Shell Nanoparticles: A Comparison with UV Photocatalysis. *Solar Energy*, **99**, 67-76. https://doi.org/10.1016/j.solener.2013.10.032

[34] Fageria, P., Gangopadhyay, S. and Pande, S. (2014) Synthesis of ZnO/Au and ZnO/Ag Nanoparticles and Their Photocatalytic Application Using UV and Visible Light. *RSC Advances*, **4**, 24962-24972. https://doi.org/10.1039/C4RA03158J

[35] Wang, X., Choi, J., Mitchell, D.R.G., Truong, Y.B., Kyratzis, I.L. and Caruso, R.A. (2013) Enhanced Photocatalytic Activity: Macroporous Electrospun Mats of Mesoporous Au/TiO_2 Nanofibers. *ChemCatChem*, **5**, 2646-2654. https://doi.org/10.1002/cctc.201300180

[36] Sun, T., Liu, E., Fan, J., Hu, X., Wu, F., Hou, W., Yang, Y. and Kang, L. (2013) High Photocatalytic Activity of Hydrogen Production from Water over Fe Doped and Ag Deposited Anatase TiO_2 Catalyst Synthesized by Solvothermal Method. *Chemical Engineering Journal*, **228**, 896-906. https://doi.org/10.1016/j.cej.2013.04.065

[37] Snyder, A., Bo, Z., Moon, R., Rochet, J.C. and Stanciu, L. (2013) Reusable Photocatalytic Titanium Dioxide-Cellulose Nanofiber Films. *Journal of Colloid and Interface Science*, **399**, 92-98. https://doi.org/10.1016/j.jcis.2013.02.035

[38] Gao, Y., Fang, P., Chen, F., Liu, Y., Liu, Z., Wang, D. and Dai, Y. (2013) Enhancement of Stability of N-Doped TiO_2 Photocatalysts with Ag Loading. *Applied Surface Science*, **265**, 796-801. https://doi.org/10.1016/j.apsusc.2012.11.114

[39] Gao, Y., Fang, P., Liu, Z., Chen, F., Liu, Y., Wang, D. and Dai, Y. (2013) A Facile One-Pot Synthesis of Layered Protonated Titanate Nanosheets Loaded with Silver Nanoparticles with Enhanced Visible-Light Photocatalytic Performance. *Chemistry—An Asian Journal*, **8**, 204-211. https://doi.org/10.1002/asia.201200768

[40] Habibi, M.H. and Sheibani, R. (2013) Nanostructure Silver-Doped Zinc Oxide Films Coating on Glass Prepared by Sol-Gel and Photochemical Deposition Process: Application for Removal of Mercaptan. *Journal of Industrial and Engineering Chemistry*, **19**, 161-165. https://doi.org/10.1016/j.jiec.2012.07.019

[41] Hebeish, A.A., Abdelhady, M.M. and Youssef, A.M. (2013) TiO_2 Nanowire and TiO_2 Nanowire Doped Ag-PVP Nanocomposite for Antimicrobial and Self-Cleaning Cotton Textile. *Carbohydrate Polymers*, **91**, 549-559. https://doi.org/10.1016/j.carbpol.2012.08.068

[42] Lekelefac, C.A., Czermak, P. and Herrenbauer, M. (2013) Evaluation of Photocatalytic Active Coatings on Sintered Glass Tubes by Methylene Blue. *International Journal of Photoenergy*, **2013**, Article ID: 614567. https://doi.org/10.1155/2013/614567

[43] Hari, M., Joseph, S.A., Mathew, S., Radhakrishnan, P. and Nampoori, V.P.N. (2012) Band-Gap Tuning and Nonlinear Optical Characterization of Ag:TiO_2 Nanocomposites. *Journal of Applied Physics*, **112**, Article ID: 074307. https://doi.org/10.1063/1.4757025

[44] Atla, S.B., Chen, C.C., Chen, C.Y., Lin, P.Y., Pan, W., Cheng, K.C., Huang, Y.M., Chang, Y.F. and Jean, J.S. (2012) Visible Light Response of Ag+/TiO_2-Ti_2O_3 Prepared by Photodeposition under Foam Fractionation. *Journal of Photochemistry and Photobiology A*: *Chemistry*, **236**, 1-8. https://doi.org/10.1016/j.jphotochem.2012.03.008

[45] Bano, I., Kumar, R.V. and Hameed, A. (2012) Influence of pH on the Preparation of Dispersed Ag-TiO_2 Nanocomposite. *Ionics*, **18**, 307-313. https://doi.org/10.1007/s11581-011-0625-4